Stable Quantum Monte Carlo Algorithm for $T = 0$ Calculation of Imaginary Time Green Functions

F.F. Assaad and M. Imada

Institute for Solid State Physics, University of Tokyo,

7-22-1 Roppongi, Minato-ku, Tokyo 106, Japan.

Abstract

We present a numerically stable Quantum Monte Carlo algorithm to calculate zero-temperature imaginary-time Green functions $G(\vec{r}, \tau)$ for Hubbard type models. We illustrate the efficiency of the algorithm by calculating the on-site Green function $G(\vec{r} = 0, \tau)$ on 4×4 to 12×12 lattices for the two-dimensional half-filled repulsive Hubbard model at $U/t = 4$. By fitting the tail of $G(\vec{r} = 0, \tau)$ at long imaginary time to the form $e^{-\tau \Delta_c}$, we obtain a precise estimate of the charge gap: $\Delta_c = 0.67 \pm 0.02$ in units of the hopping matrix element. We argue that the algorithm provides a powerful tool to study the metal-insulator transition from the insulator side.

I. INTRODUCTION

The purpose of this article is to describe a numerically stable Quantum Monte Carlo (QMC) algorithm to calculate zero-temperature imaginary time displaced Green functions:

$$G_{x,y}(\tau) = \Theta(\tau)\frac{\langle\Psi_0|c_x(\tau)c_y^\dagger|\Psi_0\rangle}{\langle\Psi_0|\Psi_0\rangle} - \Theta(-\tau)\frac{\langle\Psi_0|c_y^\dagger(-\tau)c_x|\Psi_0\rangle}{\langle\Psi_0|\Psi_0\rangle},$$

$$\text{where} \quad c_x(\tau) = e^{\tau(H-\mu N)}c_x e^{-\tau(H-\mu N)}. \tag{1}$$

Here $|\Psi_0\rangle$ denotes the ground state of the considered Hamiltonian H, $c_x^\dagger$ creates an electron with quantum numbers x, $\Theta(\tau)$ is the Heaviside function and μ is the chemical potential which has to satisfy:

$$\lim_{\beta\to\infty}\frac{\text{Tr}\left(e^{-\beta(H-\mu N)}N\right)}{\text{Tr}\left(e^{-\beta(H-\mu N)}\right)} = \frac{\langle\Psi_0|N|\Psi_0\rangle}{\langle\Psi_0|\Psi_0\rangle}, \tag{2}$$

in the zero-temperature limit $T \equiv 1/\beta \to 0$. The above equation implies that the chemical potential corresponding to the desired particle density, $n(\mu)$, has to be known prior to the simulation. In a metallic state $n(\mu)$ is in general not known a priori. However, in an insulating state at zero-temperature $n(\mu)$ is constant and in general known for chemical potentials within the charge gap Δ_c. In this situation, the here described algorithm proves to be a powerful tool. The above $T = 0$ Green functions have already been calculated with QMC methods by Deisz et al [1]. Since their algorithm does not incorporate a numerical stabilization scheme, they are restricted to relatively small values of τ (i.e. $\tau = 2.5$ in units of the hopping matrix element for the one-dimensional Hubbard model). This articles follows the work of Deisz et al. and describes a numerical stabilization scheme which allows one to calculate $T = 0$ Green functions for arbitrary values of τ.

To demonstrate the efficiency of the algorithm, we calculate $G_{x,y}(\tau)$ for the two-dimensional half-filled Hubbard model:

$$H = \sum_{\vec{i},\vec{j},\sigma} c_{\vec{i},\sigma}^\dagger T_{\vec{i},\vec{j}} c_{\vec{j},\sigma} + U\sum_{\vec{i}}\left(n_{\vec{i},\uparrow} - \frac{1}{2}\right)\left(n_{\vec{i},\downarrow} - \frac{1}{2}\right). \tag{3}$$

The quantum numbers $\vec{i}$ and σ denote lattice site and z-component of spin respectively, $n_{\vec{i},\sigma} = c_{\vec{i},\sigma}^{\dagger} c_{\vec{i}\sigma}$, and $T_{\vec{i},\vec{j}} = -t$ if $\vec{i}$ and $\vec{j}$ are nearest-neighbors. In this notation half-band filling corresponds to $\mu = 0$. As a non-trivial test of the algorithm, one may fit the tail of $G_{x,x}(\tau)$ $(x = (\vec{i}, \sigma))$ to the form $e^{-\tau \Delta_c}$ to obtain the charge gap Δ_c. At $U/t = 4$ and after extrapolation to the thermodynamic limit, our QMC data yields $\Delta_c/t = 0.67 \pm 0.02$. This value stands in good agreement with previously determined values of Δ_c [2].

The article is organized in the following way. In the next section, we briefly describe the zero-temperature auxiliary-field QMC algorithm for the Hubbard model [3–6]. We then present our solution for the numerical stabilization of the time displaced Green functions. In section 3 we describe our calculation of the charge gap for the two-dimensional Hubbard model at $U/t = 4$. In the last section, we draw some conclusions and discuss the potential applications of the algorithm.

II. THE ZERO-TEMPERATURE QMC ALGORITHM

Since the Hubbard model conserves particle number, and we are working in the canonical ensemble, one may factorize the chemical potential to obtain:

$$G_{x,y}(\tau) = \Theta(\tau) \left. \frac{\langle \Psi_0 | c_x(\tau) c_y^{\dagger} | \Psi_0 \rangle}{\langle \Psi_0 | \Psi_0 \rangle} \right|_{\mu=0} e^{\tau\mu} - \Theta(-\tau) \left. \frac{\langle \Psi_0 | c_y^{\dagger}(-\tau) c_x | \Psi_0 \rangle}{\langle \Psi_0 | \Psi_0 \rangle} \right|_{\mu=0} e^{\tau\mu}. \qquad (4)$$

Due to the above relation we consider the calculation of the $T = 0$ Green functions at $\mu = 0$.

The idea behind the zero temperature QMC algorithm is to filter out the ground state from a trial wave function $|\Psi_T\rangle$ which is required to be non-orthogonal to the ground state:

$$\frac{\langle \Psi_0 | c_x(\tau) c_y^{\dagger} | \Psi_0 \rangle}{\langle \Psi_0 | \Psi_0 \rangle} = \lim_{\Theta \to \infty} \frac{\langle \Psi_T | e^{-\Theta H} c_x(\tau) c_y^{\dagger} e^{-\Theta H} | \Psi_T \rangle}{\langle \Psi_T | e^{-2\Theta H} | \Psi_T \rangle}, \quad \tau > 0. \qquad (5)$$

The QMC calculation of

$$G_{x,y}^{>}(\Theta, \tau) \equiv \frac{\langle \Psi_T | e^{-\Theta H} c_x(\tau) c_y^{\dagger} e^{-\Theta H} | \Psi_T \rangle}{\langle \Psi_T | e^{-2\Theta H} | \Psi_T \rangle} \qquad (6)$$

proceeds in the following way. The first step is to carry out a Trotter decomposition of the imaginary time propagation:

$$e^{-2\Theta H} = \left(e^{-\Delta\tau H_t/2}e^{-\Delta\tau H_U}e^{-\Delta\tau H_t/2}\right)^m + O((\Delta\tau)^2). \tag{7}$$

Here, H_t (H_U) denotes the kinetic (potential) term of the Hubbard model and $m\Delta\tau = 2\Theta$. Having isolated the two-body interaction term, H_U, one may carry out a discrete Hubbard Stratonovitch (HS) transformation [7] to obtain:

$$e^{-\Delta\tau H_U} = C\sum_{\vec{s}}\exp\left(\sum_{x,y}c_x^\dagger D_{x,y}(\vec{s})c_y\right), \tag{8}$$

where $\vec{s}$ denotes a vector of HS Ising fields. For the Hubbard model (3), we take:

$$D_{\vec{i}\sigma,\vec{j}\sigma'}(\vec{s}) = \delta_{\sigma,\sigma'}\delta_{\vec{i},\vec{j}}\cosh^{-1}(\Delta\tau U/2)s_{\vec{i}}\sigma. \tag{9}$$

The constant $C = \exp(-\Delta\tau NU/2)/2^N$ for the N-site system will be dropped below. The imaginary time propagation may now be written as:

$$e^{-2\Theta H} = \sum_{\vec{s}}U_{\vec{s}}(2\Theta, 0) + O((\Delta\tau)^2)$$

$$\text{where} \quad U_{\vec{s}}(2\Theta, 0) = \prod_{n=1}^{m}e^{-\Delta\tau H_t/2}\exp\left(\sum_{x,y}c_x^\dagger D_{x,y}(\vec{s}_n)c_y\right)e^{-\Delta\tau H_t/2}. \tag{10}$$

In the above notation, $G_{x,y}^{>}(\Theta, \tau)$ is given by:

$$G_{x,y}^{>}(\Theta, \tau) = \frac{\sum_{\vec{s}}\langle\Psi_T|U_{\vec{s}}(2\Theta, \Theta+\tau)c_x U_{\vec{s}}(\Theta+\tau, \Theta)c_y^\dagger U_{\vec{s}}(\Theta, 0)|\Psi_T\rangle}{\sum_{\vec{s}}\langle\Psi_T|U_{\vec{s}}(2\Theta, 0)|\Psi_T\rangle} + O((\Delta\tau)^2). \tag{11}$$

The trial wave function is required to be a Slater determinant:

$$|\Psi_T\rangle = \prod_{n=1}^{N_p}\left(\sum_x c_x^\dagger P_{x,n}\right)|0\rangle. \tag{12}$$

Here N_p denotes the number of particles and P is an $N_s \times N_p$ rectangular matrix where N_s is the number of single particle states. Since $U_{\vec{s}}(2\Theta, 0)$ describes the propagation of non-interacting electrons in an external HS field, one may integrate out the fermionic degrees of freedom to obtain:

$$G_{x,y}^{>}(\Theta, \tau) = \sum_{\vec{s}}P_{\vec{s}}\left[(B_{\vec{s}}(\Theta+\tau, \Theta))G_{\vec{s}}(\Theta, \Theta)\right]_{x,y} + O((\Delta\tau)^2). \tag{13}$$

In the above equation,

$$B_{\vec{s}}(\Theta_2, \Theta_1) = \prod_{n=n_1+1}^{n_2} e^{-\Delta\tau T/2} e^{D(\vec{s_n})} e^{-\Delta\tau T/2} \quad \text{where} \quad n_1\Delta\tau = \Theta_1 \quad \text{and} \quad n_2\Delta\tau = \Theta_2,$$

$$M_{\vec{s}} = P^T B_{\vec{s}}(2\Theta, 0)P,$$

$$P_{\vec{s}} = \frac{\det(M_{\vec{s}})}{\sum_{\vec{s}} \det(M_{\vec{s}})}$$

$$\text{and} \quad (G_{\vec{s}}(\Theta, \Theta))_{x,y} = \frac{\langle \Psi_T | U_{\vec{s}}(2\Theta, \Theta) c_x c_y^\dagger U_{\vec{s}}(\Theta, 0) | \Psi_T \rangle}{\langle \Psi_T | U_{\vec{s}}(2\Theta, 0) | \Psi_T \rangle} =$$

$$\left(I - B_{\vec{s}}(\Theta, 0) P M_{\vec{s}}^{-1} P^T B_{\vec{s}}(2\Theta, \Theta) \right)_{x,y}.$$

Here I is the unit matrix, $I_{x,y} = \delta_{x,y}$. In the same notation one obtains:

$$G_{x,y}^<(\Theta, \tau) \equiv -\frac{\langle \Psi_T | e^{-\Theta H} c_y^\dagger(\tau) c_x e^{-\Theta H} | \Psi_T \rangle}{\langle \Psi_T | e^{-2\Theta H} | \Psi_T \rangle}$$

$$= \sum_{\vec{s}} P_{\vec{s}} \left[(G_{\vec{s}}(\Theta, \Theta) - I) B_{\vec{s}}^{-1}(\Theta + \tau, \Theta) \right]_{x,y}, \quad \tau > 0. \tag{14}$$

Summarizing, the zero-temperature imaginary-time Green function may be calculated from:

$$G_{x,y}(\tau) = \lim_{\Theta \to \infty} \left(\Theta(\tau) G_{x,y}^>(\Theta, \tau) + \Theta(-\tau) G_{x,y}^<(\Theta, -\tau) \right) + O((\Delta\tau)^2). \tag{15}$$

At half-band filling and due to particle hole symmetry, one may chose a trial wave function such that $P_{\vec{s}}$ is positive definite. $P_{\vec{s}}$ may be interpreted as a probability distribution and sampled with Monte-Carlo methods.

A. Numerical Stabilization

The origin of the numerical instabilities occurring in the calculation of Green functions may be understood by considering free electrons on a two-dimensional square lattice.

$$H = -t \sum_{<\vec{i},\vec{j}>} c_{\vec{i}}^\dagger c_{\vec{j}}. \tag{16}$$

Here, the sum runs over nearest-neighbors. For this Hamiltonian one has:

$$\langle \Psi_0 | c_{\vec{k}}^\dagger(\tau) c_{\vec{k}} | \Psi_0 \rangle = \exp\left(\tau(\epsilon_{\vec{k}} - \mu) \right) \langle \Psi_0 | c_{\vec{k}}^\dagger c_{\vec{k}} | \Psi_0 \rangle, \tag{17}$$

5

where $\epsilon_{\vec{k}} = -2t(\cos(\vec{k}\vec{a}_x) + \cos(\vec{k}\vec{a}_y))$, $\vec{a}_x$, $\vec{a}_y$ being the lattice constants. The chemical potential satisfies equation (2) and we will assume $|\Psi_0\rangle$ to be non-degenerate. In a numerical calculation the eigenvalues and eigenvectors of the above Hamiltonian will be known up to machine precision, ϵ. In the case $\epsilon_{\vec{k}} - \mu > 0$, $\langle\Psi_0|c_{\vec{k}}^\dagger c_{\vec{k}}|\Psi_0\rangle \equiv 0$. However, on a finite precision machine the later quantity will take a value of the order of ϵ. When calculating $\langle\Psi_0|c_{\vec{k}}^\dagger(\tau)c_{\vec{k}}|\Psi_0\rangle$ this roundoff error will be blown up exponentially and the result for large values of τ will be unreliable. In order to circumvent this problem, one may do the calculation at finite temperature and then take the limit of vanishingly small temperatures:

$$\langle\Psi_0|c_{\vec{k}}^\dagger(\tau)c_{\vec{k}}|\Psi_0\rangle = \lim_{\beta\to\infty} \frac{\exp\left(\tau(\epsilon_{\vec{k}} - \mu)\right)}{1 + \exp\left(\beta(\epsilon_{\vec{k}} - \mu)\right)}. \tag{18}$$

Even if the eigenvalues are known only up to machine precision, the right hand side of the above equation for large but finite values of β is a numerically stable operation. Although very simple, this example reflects the underlying numerical instabilities occurring in the calculation of the Green functions.

We now consider the calculation of

$$G_{\vec{s}}(\Theta + \tau, \Theta) = B_{\vec{s}}(\Theta + \tau, \Theta)G_{\vec{s}}(\Theta, \Theta) \text{ and}$$

$$G_{\vec{s}}(\Theta, \Theta + \tau) = (G_{\vec{s}}(\Theta, \Theta) - I) B_{\vec{s}}^{-1}(\Theta + \tau, \Theta) \tag{19}$$

required to compute $G_{x,y}^>(\Theta, \tau)$ (see equation (13)) and $G_{x,y}^<(\Theta, \tau)$ (see equation (14)) respectively. The equal-time Green functions, $G_{\vec{s}}(\Theta, \Theta)$, may be calculated to machine precision [4–6]. The matrices $B_{\vec{s}}(\Theta + \tau, \Theta)$ contain scales which grow and decrease exponentially with τ. As in the above example, a straightforward multiplication of both matrices will lead to numerical instabilities for large values of τ. Here, the problem is much more severe since the presence of the HS field mixes different scales. In order to circumvent this problem, we propose the following stabilization scheme.

Since the trial wave function is a Slater determinant, we can find a single particle Hamiltonian, $H_0 = \sum_{x,y} c_x^\dagger(h_0)_{x,y}c_y$, which has $|\Psi_T\rangle$ as a non-degenerate ground state. The equal time Green functions may then be written as:

$$
(G_{\vec{s}}(\Theta,\Theta))_{x,y} \equiv \frac{\langle \Psi_T | U_{\vec{s}}(2\Theta,\Theta) c_x c_y^\dagger U_{\vec{s}}(\Theta,0) | \Psi_T \rangle}{\langle \Psi_T | U_{\vec{s}}(2\Theta,0) | \Psi_T \rangle} =
$$

$$
\lim_{\beta \to \infty} \frac{\mathrm{Tr}\left(e^{-\beta H_0} U_{\vec{s}}(2\Theta,\Theta) c_x c_y^\dagger U_{\vec{s}}(\Theta,0)\right)}{\mathrm{Tr}\left(e^{-\beta H_0} U_{\vec{s}}(2\Theta,0)\right)} = \lim_{\beta \to \infty} \left(I + B_{\vec{s}}(\Theta,0) e^{-\beta h_0} B_{\vec{s}}(2\Theta,\Theta)\right)^{-1}_{x,y} \qquad (20)
$$

The last equality follows after integration of the fermionic degrees of freedom. Inspiring ourselves from the work of Hirsch [8] we calculate the time displaced Green functions in equation (19) with:

$$
\lim_{\beta \to \infty} \begin{pmatrix} I & B_{\vec{s}}(\Theta,0) e^{-\beta h_0} B_{\vec{s}}(2\Theta,\Theta+\tau) \\ -B_{\vec{s}}(\Theta+\tau,\Theta) & I \end{pmatrix}^{-1} =
$$

$$
\begin{pmatrix} G_{\vec{s}}(\Theta,\Theta) & G_{\vec{s}}(\Theta,\Theta+\tau) \\ G_{\vec{s}}(\Theta+\tau,\Theta) & G_{\vec{s}}(\Theta+\tau,\Theta+\tau) \end{pmatrix} \qquad (21)
$$

For very large but finite values of β, we can calculate the left hand side of the above equation by using matrix stabilization techniques developed for finite temperature QMC algorithms. The basic idea behind those numerical stabilization techniques is to keep the different scales occurring in the matrices $B_{\vec{s}}$ separate (for a review see reference [9]). This is achieved by decomposing the matrices $B_{\vec{s}}$ into a UDV form where U is an orthogonal matrix, D a diagonal matrix containing the exponentially large and exponentially small scales, and V a triangular matrix. The calculation of the left hand side of the above equation is done in the following way:

$$
\begin{pmatrix} I & B_{\vec{s}}(\Theta,0) e^{-\beta h_0} B_{\vec{s}}(2\Theta,\Theta+\tau) \\ -B_{\vec{s}}(\Theta+\tau,\Theta) & I \end{pmatrix}^{-1} = \begin{pmatrix} I & U_1 D_1 V_1 \\ U_2 D_2 V_2 & I \end{pmatrix}^{-1} =
$$

$$
\begin{pmatrix} V_2 & 0 \\ 0 & V_1 \end{pmatrix}^{-1} \begin{pmatrix} (V_2 U_1)^{-1} & D_1 \\ D_2 & (V_1 U_2)^{-1} \end{pmatrix}^{-1} \begin{pmatrix} U_1 & 0 \\ 0 & U_2 \end{pmatrix}^{-1} =
$$

$$
\begin{pmatrix} V_2 & 0 \\ 0 & V_1 \end{pmatrix}^{-1} (U_3 D_3 V_3)^{-1} \begin{pmatrix} U_1 & 0 \\ 0 & U_2 \end{pmatrix}^{-1}. \qquad (22)
$$

In the above equation, the matrix D_3 contains only exponentially large scales since the matrices $(V_2 U_1)^{-1}$ and $(V_1 U_2)^{-1}$ act as a cutoff to the exponentially small scales in the matrices D_2 and D_1. Since the other matrices are all well conditioned, the final matrix multiplication is well defined.

A convenient choice of H_0 is obtained in a basis where the trial wave function may be written as:

$$|\Psi_T\rangle = \prod_{n=1}^{N_p} \gamma_n^\dagger |0\rangle. \tag{23}$$

In this basis, we define H_0 through

$$H_0 \gamma_n^\dagger |0\rangle = \begin{cases} -\gamma_n^\dagger |0\rangle & \text{if } \gamma_n^\dagger \gamma_n |\Psi_T\rangle = |\Psi_T\rangle \\ +\gamma_n^\dagger |0\rangle & \text{if } \gamma_n^\dagger \gamma_n |\Psi_T\rangle = 0 \end{cases} \tag{24}$$

(Here, the energy unit is set by the hopping matrix element t.) For this choice of H_0 values of $\beta t \sim 40$ were well sufficient to satisfy equation (20) within required numerical precision [10]. The above numerical stabilization scheme was indeed successful in all examined cases.

III. EVALUATION OF THE CHARGE GAP FOR THE TWO DIMENSIONAL HUBBARD MODEL

We carried out our simulations on 4×4 to 12×12 lattices for the two-dimensional half-filled ($\mu = 0$) repulsive Hubbard model (3) at $U/t = 4$. Periodic boundary conditions were assumed. A spin singlet ground state of the kinetic energy in the Hubbard Hamiltonian was used as a trial wave function. We test the quality of this trial wave function on a 6×6 lattice. Figure 1 plots $\langle \Psi_T | e^{-\Theta H} O e^{-\Theta H} | \Psi_T \rangle / \langle \Psi_T | e^{-2\Theta H} | \Psi_T \rangle$ as a function of the projection parameter Θ for $O = S(\pi, \pi)/N = \frac{4}{3N} \sum_{\vec{r}} \exp\left(i\vec{Q}\vec{r}\right) \vec{S}(\vec{r}) \cdot \vec{S}(\vec{0})$ (solid circles in Figure 1a) and $O = E/N = H/N - U/4$ (solid circles in Figure 1b). Here $\vec{Q} = (\pi, \pi)/a$, $\vec{S}(\vec{r})$ is the spin operator on site $\vec{r}$ and N denotes the number of sites. Already for values of $\Theta t = 2.5$, both considered observables have converged within our estimated statistical uncertainty. For comparison, we have plotted $\mathrm{Tr}\left(e^{-2\Theta H} O\right) / \mathrm{Tr}\left(e^{-2\Theta H}\right)$ for the same observables (triangles

in Figure 1). Values of Θt at least twice as large are required to obtain approximate ground state results.

Another source of systematic errors comes from the discretization of the imaginary time propagation. In Table I the $\Delta\tau$ dependence of the energy and $S(\pi,\pi)$ is given. The data are obtained form the zero-temperature QMC algorithm on a 6×6 lattice and at $2\Theta t = 5$. The values at $\Delta\tau = 0$ are obtained from a least square fit of the finite $\Delta\tau$ results to the form $a + b(\Delta\tau)^2$. We carried out our simulations at $\Delta\tau t = 0.125$. As may be seen from Table I, this value of $\Delta\tau t$ produces a systematic error contained in the quoted errorbars for the energy and a systematic error of less than 1% for $S(\pi,\pi)$.

To obtain an estimate of the charge gap, we consider

$$G(\vec{r} = 0, \tau) = \frac{1}{N} \sum_x G_{x,x}(\tau), \quad \tau > 0. \tag{25}$$

Here, x stands for spin and site indices. Inserting a complete set of eigenstates of the Hamiltonian H in the $N + 1$ particle Hilbert space yields:

$$G(\vec{r} = 0, \tau) = \frac{1}{N} \sum_{n,x} |\langle \Psi_0^N | c_x | \Psi_n^{N+1} \rangle|^2 \exp\left(-\tau \left(E_n^{N+1} - E_0^N\right)\right). \tag{26}$$

where $H|\Psi_n^{N+1}\rangle = E_n^{N+1}|\Psi_n^{N+1}\rangle$ and $H|\Psi_0^N\rangle = E_0^N|\Psi_0^N\rangle$. At large values of τt, $G(\vec{r} = 0, \tau) \sim \exp\left(-\tau\Delta_c\right)$ where $\Delta_c \equiv E_0^{N+1} - E_0^N$ corresponds to the charge gap.

Our results are plotted in Figure 2. For those simulations we have chosen $\Theta t = 13.5$. Since values of τ up to $\tau_{max} t = 12$ were considered, the effective projection parameter is given by: $\Theta_{eff} = \Theta - \tau_{max}/2 = 7.5/t$. As may be seen from Figure 1, this value of the projection parameter is more than sufficient to filter out the ground state from the trial wave function. The solid lines in Figure 2 correspond to least square fits of the tail of $G(\vec{r} = 0, \tau)$ to the form $\exp(-\tau\Delta_c)$ [11]. The estimated value of the gap as a function of system size is plotted in Figure 3. A least square fit of the data to the form $a + b/L$, where L denotes the linear length of the lattice, yields $\Delta_c/t = 0.67 \pm 0.02$ in the thermodynamic limit. This value stands in good agreement with the value of the charge gap obtained by Furukawa and Imada [2]: $\Delta_c/t = 0.58 \pm 0.08$ (solid circle in Figure 3.) As may be seen from

9

the comparison of errorbars, the accuracy of the estimation has been much improved in the present study.

IV. CONCLUSIONS

We have presented an efficient, numerically stable, QMC algorithm to calculate $T = 0$ imaginary time Green functions for Hubbard type models. As a non-trivial test application of this algorithm, we have obtained an accurate estimate of the charge gap for the two-dimensional half-filled repulsive Hubbard model at $U/t = 4$: $\Delta_c/t = 0.67 \pm 0.02$.

The algorithm is formulated in the canonical ensemble. Hence, the relation $n(\mu)$ has to be known prior to the simulation. This renders the algorithm hard to use in a metallic state. However, in an insulating state at zero temperature $n(\mu)$ is constant, and generally known, for chemical potentials within the charge gap. In this situation the here presented algorithm proves to be a powerful tool. We illustrate this by considering the two-dimensional Hubbard model. Due to Equation (4), it suffices to know the Green functions at $\mu = 0$ (half-filling) to be able to determine them trivially for any other chemical potential within the charge gap. At $\mu = 0$, we are not confronted with a sign problem due to particle-hole symmetry and the statistical fluctuations do not blow-up exponentially with growing lattice sizes and projection parameters Θ. It is however clear from equation (4) that statistical fluctuations will increase (decrease) exponentially with growing positive values of τ for $\mu > 0$ ($\mu < 0$). In comparison, finite temperature algorithms in the grand-canonical ensemble, are faced with a sign problem away from $\mu = 0$. Hence, statistical fluctuations grow exponentially with growing lattice size and inverse temperature. Away from $\mu = 0$, it is thus extremely hard to extrapolate any zero temperature result from the finite temperature grand-canonical algorithms for large lattice sizes. This renders the here presented algorithm a powerful tool for the study of the metal-insulator transition from the insulator side [13].

ACKNOWLEDGEMENTS

REFERENCES

[1] J.J. Deisz, W. von der Linden, R. Preuss and W. Hanke, to appear in *Computer simulations in Condensed Matter Physics VIII*, Eds. D.P. Landau, K.K. Mon and H.B. Schüttler (Spinger Verlag, Heidelberg, Berlin, 1995)

[2] N. Furukawa and M. Imada, J. Phys. Soc. Jpn. **61** (1992) 3331.

[3] G. Sugiyama and S.E. Koonin, Anals of Phys.**168** (1986) 1.

[4] S. Sorella, S. Baroni, R. Car, And M. Parrinello, Europhys. Lett. **8** (1989) 663. S. Sorella, E. Tosatti, S. Baroni, R. Car, and M. Parinello, Int. J. Mod. Phys. B**1** (1989) 993.

[5] M. Imada and Y. Hatsugai, J. Phys. Soc. Jpn. **58** (1989) 3752.

[6] F.F. Assaad, Helvetica Pysica Acta **63** (1990) 580.

[7] J.E.Hirsch, Phys. Rev. B. 28 (1983) 4059.

[8] J.E. Hirsch, Phys. Rev. B **38** (1988) 12023.

[9] E. Loh and J. Gubernatis, in Modern Problems of Condensed Matter Physics, edited by W. Hanke and Y.V. Kopaev, (North Holland, Amsterdam, 1992), Vol 32, p. 177.

[10] On average equation (20) was satisfied up to 10^{-11} in absolute values.

[11] Since the statistical fluctuations for different values of τ are not independent, we have done our error analysis in a basis where the covariance matrix is diagonal (see reference [12])

[12] M. Jarrel and J.E. Gubernatis, *Bayesian Inference and the Analytic Continuation of Imaginary-Time Quantum Monte Carlo Data*. Preprint.

[13] F.F. Assaad and M. Imada, unpublished.
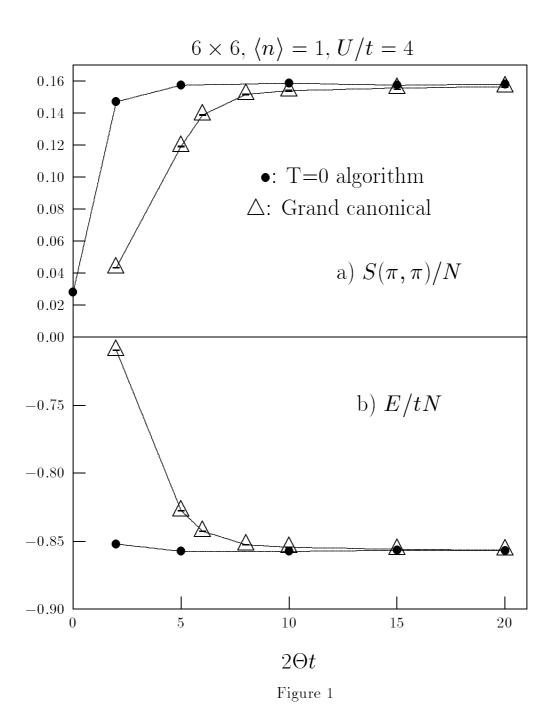
Figure captions

Fig. 1 •: $\langle\Psi_T|e^{-\Theta H}Oe^{-\Theta H}|\Psi_T\rangle/\langle\Psi_T|e^{-2\Theta H}|\Psi_T\rangle$ as a function of the projection param-
eter Θ. The trial wave function is a singlet ground state of the kinetic energy in
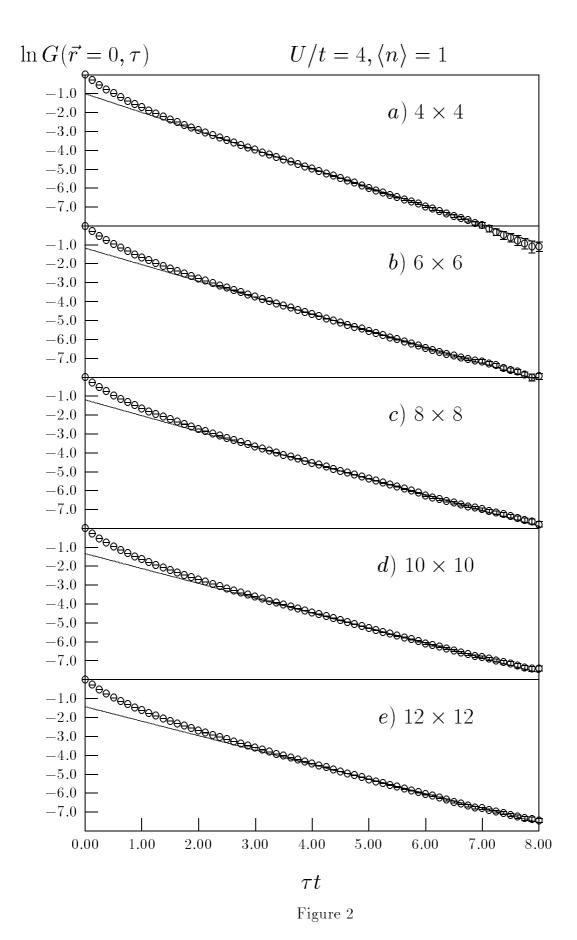Hubbard Hamiltonian. △: $\mathrm{Tr}\left(e^{-2\Theta H}O\right)/\mathrm{Tr}\left(e^{-2\Theta H}\right)$.
We have considered two observables: a)$O = S(\pi,\pi)/N$, b) $O = E/N$.

Fig. 2 $\ln G(\vec{r}=0,\tau)$ as a function of lattice size. The solid lines are least square fits
of the tail of $G(\vec{r}=0,\tau)$ to the form $e^{-\tau\Delta_c}$.

Fig. 3 Δ_c as a function of $1/L$ where L corresponds to the linear size of the square lat-
tice. The solid circle at $1/L = 0$ corresponds to Furukawa and Imada's estimate
of Δ_c (see reference [2]).

TABLES

TABLE I. Energy per site and $S(\pi, \pi)$ as a function of $\Delta\tau t$ for the Hubbard model at $U/t = 4$ on a 6×6 lattice. The simulations were carried out with the zero-temperature QMC algorithm at $2\Theta t = 5$. The quoted values at $\Delta\tau t = 0$ are obtained from a least square fit to the form $a + b(\Delta\tau t)^2$

$\Delta\tau t$	E/Nt	$S(\pi, \pi)/N$
0.0	-0.8575 ± 0.0003	0.1579 ± 0.0007
0.0625	-0.8571 ± 0.0004	0.1578 ± 0.0009
0.1	-0.8571 ± 0.0003	0.1570 ± 0.0006
0.125	-0.8570 ± 0.0003	0.1564 ± 0.0007
0.166	-0.8563 ± 0.0003	0.1557 ± 0.0008

6×6, $\langle n \rangle = 1$, $U/t = 4$

$\bullet$: T=0 algorithm

$\triangle$: Grand canonical

a) $S(\pi, \pi)/N$

b) E/tN

$2\Theta t$

Figure 1

$\ln G(\vec{r} = 0, \tau)$ $\qquad$ $U/t = 4, \langle n \rangle = 1$

a) 4×4

b) 6×6

c) 8×8

d) 10×10

e) 12×12

τt

Figure 2

Δ_c/t

$U/t = 4, \langle n \rangle = 1$

$1/L$

Figure 3